## Immune cell imaging using Multi-Spectral Optoacoustic Tomography (MSOT)

Stratis Tzoumas<sup>1,†</sup>, Angelika Zaremba<sup>1,†</sup>, Uwe Klemm<sup>1</sup>, Antonio Nunes<sup>1</sup>, Karin Schaefer<sup>1</sup>, Vasilis Ntziachristos <sup>1,\*</sup>

<sup>1</sup> Institute for Biological and Medical Imaging (IBMI), Technische Universität München and Helmholtz Zentrum München, German Research Center for Environment and Health, Ingolstädter Landstrasse 1, 85764 Neuherberg, Germany <sup>†</sup>These authors contributed equally to this work.

\*Corresponding author: v.ntziachristos@tum.de

Received Month X, XXXX; revised Month X, XXXX; accepted Month X, XXXX; posted Month X, XXXX (Doc. ID XXXXX); published Month X, XXXX

Multi-spectral optoacoustic tomography offers the potential to image in high resolution cells tagged with optical labels. In contrast to single wavelength imaging, multispectral excitation and spectral unmixing can differentiate labeled moieties over tissue absorption in the absence of background measurements. This feature can enable longitudinal cellular biology studies well beyond the depths reached by optical microscopy. However the relation between spectrally resolved fluorescently labeled cells and optoacoustic detection has not been systematically investigated. Herein we measured titrations of fluorescently labeled cells and establish the optoacoustic signal generated by fluorescent labeled cells as a function of cell number and across different cell types. We then assess the MSOT sensitivity to resolve cells implanted in animals. OCIS Codes: (170.5120) Photoacoustic imaging; (170.3880) Medical and biological imaging, (170.1530) Cell analysis. http://dx.doi.org/10.1364/OL.99.099999

Microscopy plays a critical role in cell biology, enabling observations of cell-cell and cell-host interactions in vivo [1]. However the limited penetration of microscopy methods only allows superficial observations. Many applications however require cell imaging at different scales. Recent cell-based therapy studies for example, such as cell-based cancer immunotherapy and stem cell treatment, have shown the potential of cell therapy to develop into a novel therapeutic platform. Various therapeutic cell types, such as T cells, dendritic cells and natural killer cells are administered to cancer patients after ex vivo manipulation to target and inhibit tumor growth with significantly less side effects on normal cells [2]. Likewise macrophages have been considered for treating cancer, fibrosis and inflammation [3-5]. However, the assessment of therapeutic cell bio-distribution largely relies on ex vivo examinations. As a result, the migration and targeting of cells and underlying dynamic processes have not yet been fully elucidated, even if critical for understanding the mechanisms leading to successful treatment.

Imaging methods that allow the macroscopic visualization of cell bio-distribution through entire living organisms have been considered, but come with their own limitations. The most popular modality, bioluminescence imaging (BLI), is fundamentally limited from lack of quantification. The signal recorded in bioluminescence imaging is a surface-weighted low resolution photon intensity signal with limited ability to accurately resolve its spatial origin in three-dimensions or relate this signal to the number of cells generating it. Fluorescence epiillumination imaging (FEI) comes with limitations. Diffuse optical tomography approaches and nuclear imaging methods such as fluorescence molecular tomography (FMT) or Positron Emission Tomography

respectively have also been considered. They typically offer three-dimensional imaging ability and better quantification capacity over BLI or FEI but are similarly limited by resolution that is no better than 1 mm in small animals and become worse in larger animals. Overall, nuclear imaging techniques are further limited by the need to employ radio-isotopes which decay and do not enable long-term observations. Conversely optical methods such as FMT allow for longitudinal studies but are less sensitive to nuclear methods, in particular as the depth of the activity increases. High resolution radiologic methods such MRI and X-ray CT are less frequently regarded for imaging cells due to their low sensitivity.

With the advent of multi-spectral optoacoustic tomography (MSOT), there are novel possibilities for macroscopic cell imaging. MSOT can offer high-resolution optical detection in three-dimensions and extends the penetration of conventional microscopy into the mesoscopic regime exchanging resolution to depth. The ability to image un-labeled, highly absorbing cells [6] or cells labeled with fluorescent proteins and nanoparticles has been already demonstrated [7-9]. However no systematic study has been so far performed to assess the MSOT sensitivity in immune cell imaging.

In this work we take a first step toward relating MSOT signals to the spectrally resolved absorption properties of labeled immune cells. A particular MSOT feature is the use of multi-wavelength illumination and the application of spectral unmixing techniques to capture the spectra of different absorbing moieties. Recently we have reported on the use of statistical sub-pixel detection techniques [10] yielding sensitive and accurate MSOT sensing, beyond the capacity of linear unmixing methods. Of particular importance herein was to identify the sensitivity of MSOT combined with appropriate spectral processing methods

for the application of cell imaging. We employ these methods herein, for understanding the detection ability for cells labeled with fluorescent dyes. From an optoacoustic detection stand-point, fluorescence labels present perhaps a worst case scenario for cell imaging with MSOT over other labeling methods, such as using gold nanoparticles [11]. From a biology point of view however fluorescence labels are better established and characterized. Importantly, fluorescent labels come with the advantage that the cells can be also visualized by traditional optical methods, for example fluorescence microscopy, to better understand the loading and other biological parameters.

For MSOT measurements we employed a state of the art 256 channel real-time imaging MSOT scanner (iThera Medical GmbH, Kreiling Germany). The general characteristics of a similar 64-channel system have been described elsewhere [12]. The system employs an OPO tunable laser for illumination in the NIR and parallel detection of 256 channels to achieve fast, real-time imaging. Two types of cells were employed in the studies to examine the effects of cell variability. Jurkat T cells were grown in RPMI 1640 media (Invitrogen # 31870074) containing 10% FBS, 2mM L-Glutamine, 1mM Sodium-Pyruvate, non-essential amino acids and penicillinstreptomycin. In addition, J774A.1 mouse macrophages were cultured in RPMI 1640 media including 10 % FBS and penicillin-streptomycin. Cells were labeled with the near-infrared fluorescent cyanine dve 1,1'-Dioctadecyl-3,3,3',3'-Tetramethylindotricarbocyanine Iodide (DiR) for optoacoustic detection. DiR is a lipophilic, near-infrared fluorescent cyanine dye that can be incorporated into the cell membrane. For labelling 1x106 cells were incubated with DiR for 15 min at room temperature while mixing every 5 min. Optimal labeling results were determined by testing different DiR concentrations and monitoring cell viability using MTT assay (Roche Applied Science, Penzberg Upper Bavaria, Germany) according to the manufacturer's instruction. Optimal labeling of the J774A.1 macrophage cell line was achieved using 10 uM DIR leading to an overall labeling of about 99,6% of cells  $(SD \pm 0.58\%)$  and a cell viability of 97 %. Optimal labeling of Jurkat cells was found when using 5 µM DIR, which lead to an overall labeling of 97,6% (SD  $\pm$  1,23%) and a cell viability of about 91 %. The degree of cell labeling was determined by counting fluorescence positive cells in the overlay with the DIC image (n=4).

MSOT cell imaging in vitro. Cells were first imaged *invitro* by utilizing 2cm-diameter cylindrical phantoms made of 1.3% Agar (Sigma-Aldrich) and 1.2% by volume of Intralipid emulsion (Sigma-Aldrich) leading to an optically diffusive medium with acoustic properties similar those of tissue. The use of an absorption-less phantom was selected herein to explicitly study the signal contribution of only the labelled cells. Measurements in animals then provided a reference medium with tissue absorption for comparison purposes. The labeled cells were enclosed within a 3mm diameter plastic tube implanted into the agar cylinder, as shown in Fig. 1-A. Both Jurkat cells (Fig. 1-B) and J774A.1 cells (Fig. 1-C) were imaged using exactly the same imaging parameters. The labeled cells were enclosed within a 3mm diameter

plastic tube implanted into the agar cylinder, as shown in Fig.1-A. Three different labeled cell concentrations were inserted into the 3mm tubes, corresponding to 1250, 2500 and 5000 cells in the volume imaged. Unlabeled cells were also imaged as control (Fig. 1). MSOT imaging was performed in one imaging plane (~ 200 µm in plane resolution, ~800 µm cross-section). The phantom images were reconstructed at a wavelength of 720nm where the DiR signal is prominent (Fig. 1 B (i-iii), Fig. 1-C (i-iii)). Overall, a linear increase in signal intensity with increasing cell number is observable (Fig. 1 B-(iv), Fig. 1-C (iv)), as it is theoretically expected.

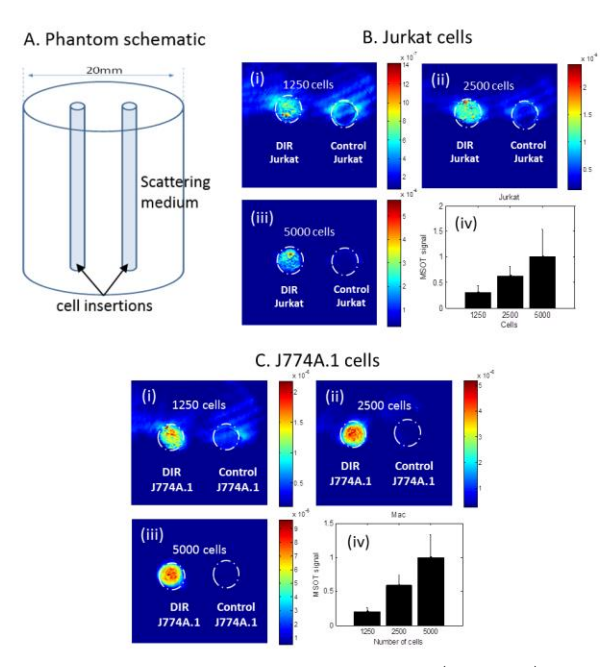


Fig. 1. In vitro optoacoustic imaging (720 nm) of DiR labeled cells. A. Schematic illustration of the phantoms used in the in vitro tests. Labeled and unlabeled cells are inserted in 3mm diameter tubes that are placed within a 20mm diameter scattering phantom. B. Imaging of Jurkat cells. (i) – (iii) Optoacoustic signal generated by 1250. 2500 and 5000 DiR labelled cells, respectively. (iv) Opotacoustic signal intensity comparison for different amounts of labeled cells. The bar heights indicate the mean intensity within the region of interest and the error bars indicate the standard deviation. C. Imaging of J774A.1 cells. (i) - (iii) Optoacoustic signal generated by 1250, 2500 and 5000 DiR labelled J774A.1 cells, respectively. (iv) Opotacoustic signal comparison for different amounts of labeled cells. The bar heights indicate the mean intensity within the region of interest and the error bars indicate the standard deviation.

The relative absorbance of labeled cells was characterized using the same scattering phantom as the one described in Fig. 1-A. For contrasting the signal obtained from labeled cells with a well characterized absorption signal we employed India ink for reference measurements. In particular, labeled Jurkat (Fig. 2 (a)) and J774A.1 cells (Fig. 2 (b)) were sequentially imaged next to an insertion of black India ink with an absorbance of  $\mu_{\alpha} = 0.5$  cm<sup>-1</sup>, the latter determined by a

photospectrometer. Imaging was performed at 720 nm using MSOT. The optoacoustic signal intensity produced by 5000 Jurkat (Fig. 2 (a)) and J774A.1 cells (Fig. 2 (b)) was imaged together with an identical amount of ink. We observed that the optoacoustic signal produced by J774A.1 cells was almost twice as high as the one produced by Jurkat cells (Fig. 2 (c)). To explain this difference we measured the cell sizes and found that macrophages had larger diameter compared to the T cell line (Fig. 2 (d)):  $J774A.1 = 17,94 \mu m$ ,  $SD \pm 1,99$ ; Jurkat =13,44 µm, SD  $\pm$  2,1; (statistics stemming after counting n=47 cells per cell line using the "Leica Application Suite" software). The larger cell diameter of the J774A.1 cells indicates an almost double cell surface which indicates double DiR concentration per cell and can explain the optoacoustic signal measured (Fig. 2(c)).

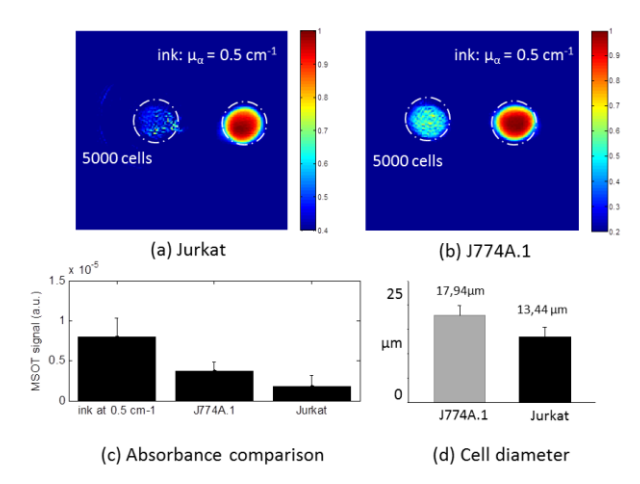


Fig. 2. Comparison and quantification of the absorbance of DiR labelled cells. (a,b) Single-wavelength (720nm) optoacoustic phantom images of 5000 DiR labeled Jurkat cells (a) and J774A.1 cells (b) next to black India ink of absorption coefficient 0.5 cm<sup>-1</sup>. (c) Comparison in terms of optoacoustic signal intensity between the ink reference and the 5000 Jurkat and J774A.1 cells. (d) Comparison of the cell diameter of Jurkat and J774A.1 cells.

highly cells are scattering photospectrometry a non-ideal method for estimating their absorbance in absolute values. Optoacoustic imaging can serve as a better alternative in this respect. Assuming that the differences in Grüneissen coefficient are insignificant, we can quantify the absolute absorbance of the labeled cells through the comparison with the black India ink. Specifically, based on Fig. 2 (c), we found that 5000 Jurkat cells produce an optoacoustic signal that corresponds to  $\mu_{\alpha}$  of ~0.12 cm<sup>-1</sup>, and 5000 J774A.1 cells to  $\mu_{\alpha}$  of ~0.25 cm<sup>-1</sup>. Using this information and the linear signal response as a function of cell number (Fig. 1), we can approximately estimate the absorbance as a function of the number of cells. Knowing that tissue absorption in the NIR ranges in the area of 0.4 to 0.1 cm<sup>-1</sup> [13], we hypothesize that in order to produce enough contrast for accurate MSOT sensing, cell clusters in the range of 1,000-10,000 would be required.

**Animal imaging.** To confirm the theoretical prediction and the overall ability to detect labeled immune cells in

tissues, we selected the cell line with the stronger labeling ability in order to provide first insights into the MSOT sensitivity for fluorescently labeled cells. We performed two experiments. In each experiment we injected two different amounts of cells in the left (injection 1) and the right brain hemisphere (injection 2) of a euthanized mouse. In experiment A we injected locally 25,000 J774A.1 cells in the left and 10,000 J774A.1 cells in the right brain hemisphere. In experiment B we injected locally 5,000 J774A.1 cells in the left and 2,500 J774A.1 cells in the right brain hemisphere. Mice were euthanized before cell injection and then imaged using MSOT. After MSOT imaging, the mice were imaged using cryoslicing fluorescence imaging [14] to verify the position of the cell insertions. Euthanasia was performed according to procedures approved by local subcommittee on animal research.

For MSOT imaging, the mice were placed horizontally on a thin polyethylene membrane and placed within the MSOT scanner. Sound coupling and animal temperature maintenance was achieved by surrounding the membrane with water actively controlled at 34°C. Excitation wavelengths from 700 nm to 900 nm in steps of 10nm were collected. MSOT images were reconstructed for each wavelength using a model-based reconstruction algorithm [15]. Afterwards, the cell bio-distribution was spectrally resolved from the absorbing tissue background using the measured spectrum of the labeled cells and Adaptive Matched Filter as in [10]. After the completion of each MSOT measurement, the mice were frozen and tissue slices were photographed and imaged with a fluorescence The fluorescence measurements superimposed in green pseudocolor on the color images. The fluorescence cryoslice images are shown next to the MSOT images for validation purposes.

Fig. 3 depicts the results from the experiments A and B. In each case, the cell insertions are explicitly pointed with white arrows. Fig. 3 (a), (b) correspond to experiment A and Fig. 3 (c), (d) to experiment B. Fig. 3 (a) presents an overlay of the J774A.1 cell bio-distribution as detected using MSOT/AMF unmixing (red) on the anatomical optoacoustic image at 900 nm. Fig. 3 (b) shows a corresponding fluorescence cryoslice image, which confirms the results of the non-invasive MSOT image. We note that the signals captured by fluorescence imaging are generally of lower resolution (due to photon diffusion) compared to the MSOT images and some minor disagreement is expected. Fig. 3 (c) demonstrates imaging of macrophages at 5,000 and 2,500 amounts. In all cases the signals are reliably detected.

Our data show that the J774A.1 macrophages were detectable in *ex vivo* mice via MSOT in all four titrations, from 25,000 to 2,500 cells. Retrospect analysis based on the signal to noise characteristics of these four measurement points indicates that sensitivities of the order of 1000 cells or less may be possible. However, an exact determination of sensitivity is best performed on a per case basis. The MSOT sensitivity depends on multiple parameters including system parameters, in particular the light intensity deposited on tissue, the detector sensitivity, the excitation wavelengths employed and the spectral unmixing method utilized. It further depends on

the depth of the cell activity and the optical properties of tissue. A third dependence of the sensitivity is on the lesion size. Cells distributing over a larger volume will generally generate lower ultrasound frequencies than cells accumulating in smaller lesions. Since higher ultrasound frequencies attenuate more strongly than lower frequencies, the detection of cells over very small volumes will be more challenging. Finally a fourth dependence is on the particular label employed.

We should note that it is common to determine optoacoustic sensitivity by multiplying the total number of cells imaged with the ratio of the volume of the optoacoustic voxel over the total volume that the cells are distributed in. This gives some very favorable sensitivity numbers which may be rather inaccurate. This is because, as mentioned, a very small volume emits an optoacoustic signal of much higher frequency content which is attenuated more strongly than the lower frequency signals emitted from a larger volume. This non-linear relationship of sensitivity with volume has been shown before [16]. Instead sensitivity should be demonstrated on a per case and actual distribution volume or by using models that account for this non-linear behavior.

The demonstration of experimentally detecting at least ~2,500 cells from a small volume inside tissue gives a first indication of MSOT as a cell imaging method. An important additional parameter that will affect sensitivity is the labeling approach employed. Herein we selected a fluorescent label that is commonly employed for cell imaging applications and binds to the surface of the cells. We observe that the size of the cell surface plays an important role on the optoacoustic signal generated and smaller cells may be more challenging in detection. Alternative labels, like gold nanoparticles, potentially improve the detection sensitivity. However, the ability to offer better detection characteristics with nanoparticles should be explicitly demonstrated, as it also associates with the labeling efficiency - i.e. how many particles can be uptaken by the cell type of interest.

In summary, we have demonstrated for the first time the ability of MSOT to image within tissue, leukocytes labeled with a fluorescent dye. Of particular importance was the identification of sensitivity metrics as it relates to biological exploration. For this reason signals obtained from labeled cells were first contrasted to signals obtained from characterized amounts of India ink. Then measurements from animals were obtained to interrogate the ability and sensitivity to resolve cells in tissues.

Acknowledgements: All animal experiments were approved by the District Government of Upper Bavaria. We thank the groups of Prof. Angela Krackhardt, Technische Universität München, Germany, for providing the Jurkat cells. We further acknowledge support from EU project FAMOS (FP7 ICT, Contract 317744) (Spectral algorithms), the Federal Ministry of Education and Research, Photonic Science Germany (Tech2See-13N12624) (Cell labeling) the ERC Advanced Grant (233161) (MSOT development).

## References

 J. Condeelis and J. E. Segall, Nat Rev Cancer, 3, 921 (2003)

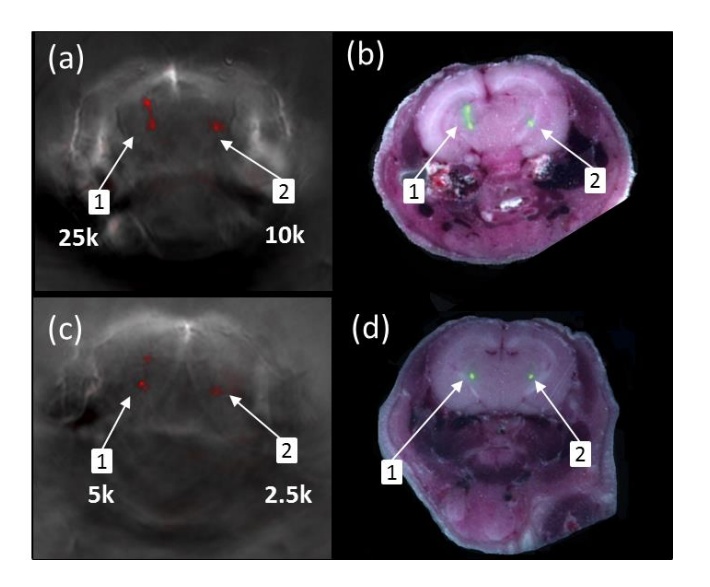


Fig. 3. Ex vivo animal study. (a,c) Overlay of the spectrally resolved signal stemming from the DiR labelled J774A.1 cells (red color) onto the anatomical optoacoustic image (at 900 nm) for experiments A and B respectively. The white arrows indicate the positions of the cell insertions. (b,d) Overlay of the fluorescent signal stemming from the DiR labelled cells (green color) onto the anatomical cryoslice image for experiments A and B, respectively.

- 2. N. P. Restifo, M. E. Dudley, and S. A. Rosenberg, Nature Reviews Immunology, **12**, 269 (2012).
- H. Liu, X. Wu, S. Wang, W. Deng, L. Zan, and S. Yu, Oncol Res, 20, 275 (2013).
- J. A. Thomas, C. Pope, D. Wojtacha, A. J. Robson, T. T. Gordon-Walker, S. Hartland, P. Ramachandran, M. Van Deemter, D. A. Hume, J. P. Iredale, and S. J. Forbes, Hepatology, 53, 2003 (2011).
- 5. D. Ferenbach and D. Kluth, Semin Nephrol, 30, 345 (2010).
- 6. E. M. Strohm, E. S. Berndl, and M. C. Kolios, Photoacoustics, 1, 49 (2013).
- D. Razansky, M. Distel, C. Vinegoni, R. Ma, N. Perrimon, R. W. Koster, and V. Ntziachristos, Nat. Photon., 3, 412 (2009).
- 8. A. Taruttis, M. Wildgruber, K. Kosanke, N. Beziere, K. Licha, R. Haag, M. Aichler, A. Walch, E. Rummeny, and V. Ntziachristos, Photoacoustics, 1, 3 (2013).
- 9. S. Y. Nam, L. M. Ricles, L. J. Suggs, and S. Y. Emelianov, *PLoS One*, **7**, e37267 (2012).
- S. Tzoumas, N. Deliolanis, S. Morscher, and V. Ntziachristos, IEEE Trans. Med. Imaging, 33, 48 (2014).
- P. P. Joshi, S. J. Yoon, Y.-S. Chen, S. Emelianov, and K. V. Sokolov, Biomed. Opti. Express, 4, 2609 (2013).
- 12. A. Buehler, E. Herzog, D. Razansky, and V. Ntziachristos, Opt. Lett., **35**, 2475 (2010).
- S. L. Jacques, Physics in medicine and biology, 58, R37 (2013).
- A. Sarantopoulos, G. Themelis, and V. Ntziachristos, Molecular Imaging and Biology, 13, 874 (2011).
- A. Rosenthal, D. Razansky, and V. Ntziachristos, IEEE Trans. Med. Imaging, 29, 1275 (2010).
- 16. D. Razansky, J. Baeten, and V. Ntziachristos, Medical Physics, 36, 939 (2009).

## Full References.

- J. Condeelis and J. E. Segall, "Intravital imaging of cell movement in tumours," *Nat Rev Cancer*, vol. 3, pp. 921-930, 2003.
- 2. N. P. Restifo, M. E. Dudley, and S. A. Rosenberg, "Adoptive immunotherapy for cancer: harnessing the T cell response," *Nature Reviews Immunology*, vol. 12, pp. 269-281, 2012.
- 3. H. Liu, X. Wu, S. Wang, W. Deng, L. Zan, and S. Yu, "In vitro repolarized tumor macrophages inhibit gastric tumor growth," *Oncol Res,* vol. 20, pp. 275-80, 2013.
- 4. J. A. Thomas, C. Pope, D. Wojtacha, A. J. Robson, T. T. Gordon-Walker, S. Hartland, P. Ramachandran, M. Van Deemter, D. A. Hume, J. P. Iredale, and S. J. Forbes, "Macrophage therapy for murine liver fibrosis recruits host effector cells improving fibrosis, regeneration, and function," *Hepatology*, vol. 53, pp. 2003-15, Jun 2011.
- D. Ferenbach and D. Kluth, "Macrophage cell therapy in renal disease," *Semin Nephrol*, vol. 30, pp. 345-53, May 2010.
- E. M. Strohm, E. S. Berndl, and M. C. Kolios, "High frequency label-free photoacoustic microscopy of single cells," *Photoacoustics*, vol. 1, pp. 49-53, 2013.
- 7. D. Razansky, M. Distel, C. Vinegoni, R. Ma, N. Perrimon, R. W. Koster, and V. Ntziachristos, "Multispectral opto-acoustic tomography of deepseated fluorescent proteins in vivo," *Nat Photon*, vol. 3, pp. 412-417, 2009.
- 8. Taruttis, M. Wildgruber, K. Kosanke, N. Beziere, K. Licha, R. Haag, M. Aichler, A. Walch, E. Rummeny, and V. Ntziachristos, "Multispectral optoacoustic tomography of myocardial infarction," *Photoacoustics*, vol. 1, pp. 3-8, 2013.
- 9. S. Y. Nam, L. M. Ricles, L. J. Suggs, and S. Y. Emelianov, "In vivo ultrasound and photoacoustic monitoring of mesenchymal stem cells labeled with gold nanotracers," *PLoS One*, vol. 7, p. e37267, 2012.
- S. Tzoumas, N. Deliolanis, S. Morscher, and V. Ntziachristos, "Unmixing Molecular Agents From Absorbing Tissue in Multispectral Optoacoustic Tomography," *IEEE Trans. Med. Imaging*, vol. 33, p. 48, 2014.
- P. P. Joshi, S. J. Yoon, Y.-S. Chen, S. Emelianov, and K. V. Sokolov, "Development and optimization of near-IR contrast agents for immune cell tracking," *Biomedical optics express*, vol. 4, pp. 2609-2618, 2013.
- Buehler, E. Herzog, D. Razansky, and V. Ntziachristos, "Video rate optoacoustic tomography of mouse kidney perfusion," *Opt Lett*, vol. 35, pp. 2475-2477, 2010.
- S. L. Jacques, "Optical properties of biological tissues: a review," *Physics in medicine and biology*, vol. 58, p. R37, 2013.
- Sarantopoulos, G. Themelis, and V. Ntziachristos, "Imaging the bio-distribution of fluorescent probes using multispectral epi-illumination cryoslicing imaging," *Molecular Imaging and Biology*, vol. 13, pp. 874-885, 2011.
- 15. Rosenthal, D. Razansky, and V. Ntziachristos, "Fast semi-analytical model-based acoustic inversion for

- quantitative optoacoustic tomography," *IEEE Trans Med Imaging*, vol. 29, pp. 1275-85, Jun 2010.
- D. Razansky, J. Baeten, and V. Ntziachristos, "Sensitivity of molecular target detection by multispectral optoacoustic tomography (MSOT)," Medical Physics, vol. 36, p. 939, 2009.